

Supporting Information for:

Orchestration of Enzymatic Processing by Thiazole/Oxazole-Modified Microcin Dehydrogenases

Joel O. Melby^{1,2}, Xiangpo Li^{1,2}, and Douglas A. Mitchell^{1-3*}

¹ Department of Chemistry, ² Institute for Genomic Biology, and ³ Department of Microbiology; University of Illinois at Urbana-Champaign; Urbana, Illinois, 61801; USA

*Corresponding author; Mitchell, Douglas A. (douglasm@illinois.edu), phone: 1-217-333-1345, fax: 1-217-333-0508)

Table S1	Oligonucleotides used in this study
Table S2	Bioinformatic data for the dehydrogenases used in this study
Figure S1	Dehydrogenase identity/similarity matrix and amino acid sequence of precursor peptides
Figure S2	Three potential pathways for azole formation in ribosomal natural product biosynthesis
Figure S3	The order of azole formation on BalhA1-5Tzn by CmsB and BamB
Figure S4	Minimal requirement for dehydrogenase activity
Figure S5	Noncognate dehydrogenase activity towards BalhA1-5Tzn
Figure S6	TOMM dehydrogenase alignment
Figure S7	Non-TOMM dehydrogenase crystal structure highlighting the Lys-Tyr motif
Figure S8	UV/Vis of dehydrogenases
Figure S9	McbC-K201A and -Y202A lack dehydrogenase activity
Figure S10	Binding of BcerB-K185A/Y186A to BalhC/D
Figure S11	The reduction potential of McbC as measured by phenosafranine titration

Oligonucleotide	Sequence
CmsB f (BamHI)	AAAAG <i>GATCC</i> ATGAGCACCATCGAGACCGACGC
CmsB r (NotI)	AAAAG <i>CGGCCGCT</i> CAGTCATGGGAGGCCTCCTCGTC
BamB f (BamHI)	AAAAG <i>GATCC</i> ATGAAAGAGATTGAAAGGCATGCCACTAATTTGG
BamB r (NotI)	AAAAG <i>CGGCCGCT</i> CATGTTCTGCAACTAAAGTATATATAGGGGCATC
SaciB f (Sall)	AAAAG <i>TGACA</i> AATTGAATCCTTTTTGAGAGGTTTTATCTAGATAC
SaciB r (NotI)	AAAAG <i>CGGCCGCT</i> CATTCTCTCCCACTACCAA
BcerB-K185A f	GCCAATCTTGATCAAACAAGTAGT <i>GCATACGC</i> CAGATAGGGGATATAAGTT
BcerB-K185A r	AACTTATATCCCCTATCTGCGTAT <i>GCACTACT</i> TGTTTGATCAAGATTGGC
BcerB-Y186A f	CTGCCAATCTTGATCAAACAAGTAGTAAAG <i>CCGC</i> CAGATAGGGGATA
BcerB-Y186A r	TATCCCCTATCTG <i>CGGCT</i> TTACTACTTGTTTGATCAAGATTGGCAG
SaciB-K173A f	TTTACTGGAAGCCGATGGTT <i>GCATATG</i> GAAATAGAGGAGCCAG
SaciB-K173A r	CTGGCTCCTCTATTTCCATAT <i>GCA</i> ACCATCGGCTTCCAGTATAA
SaciB-Y174A f	CTTACTGGAAGCCGATGGTTAAAG <i>CT</i> GAAATAGAGGAGCCAG
SaciB-Y174A r	CTGGCTCCTCTATTTCC <i>AGCT</i> TTAACCATCGGCTTCCAGTATAAG
BcerB-K185A/Y186A f	GCCAATCTTGATCAAACAAGTAGT <i>GCAGCCGC</i> CAGATAGGGGATA
BcerB-K185A/Y186A r	TATCCCCTATCTG <i>CGGCTGC</i> ACTACTTGTTTGATCAAGATTGGC
SaciB-K173A/Y174A f	TTACTGGAAGCCGATGGTT <i>GCAGCT</i> GAAATAGAGGAGCC
SaciB-K173A/Y174A r	GGCTCCTCTATTTCC <i>AGCTGCA</i> ACCATCGGCTTCCAGTATA

Table S1. Oligonucleotides used in this study. The direction the primer binds the particular gene are described as forward (f) and reverse (r). The restriction site for primers used for cloning are provided in parenthesis, while the restriction sequence is bolded and italicized. Primers used for site-directed mutagenesis have the mutated codon(s) underlined.

Dehydrogenase	Locus Tag	GI number	Organism	%Identity/%Similarity to BalhB
BcerB	bcere0005_53170	228601410	<i>Bacillus cereus</i> 172560W	78/94
BamB	RBAM_007480	154685203	<i>Bacillus amyloliquefaciens</i> FZB42	19/60
CmsB	Cms_0547	170780985	<i>Clavibacter michiganensis</i> subsp. <i>sepedonicus</i>	16/51
McbC	MCBC_ECOLX	126808	<i>Escherichia coli</i>	16/59
PagB	PF0001	18891897	<i>Pyrococcus furiosus</i> DSM 3638	21/61
SaciB	Saci_0525	70606348	<i>Sulfolobus acidocaldarius</i> DSM 639	23/66

Table S2. Bioinformatic data for the dehydrogenases used in this study. Shown are the dehydrogenase designations, along with their respective locus tags, GI numbers, producing organism, and percent identity/similarity to BalhB. The dehydrogenase responsible for microcin B17 biosynthesis (*E. coli*) was assigned a letter designation for its position within the biosynthetic gene cluster, not its function.

A

Dehydrogenase	BalhB	BcerB	McbC	SagB	ClosB	BamB	CmsB	SaciB	PagB
BalhB	100	94	59	60	62	60	51	66	61
BcerB	78	100	58	56	60	63	60	57	59
McbC	16	12	100	61	61	60	62	52	56
SagB	15	16	13	100	81	62	54	65	64
ClosB	21	19	18	40	100	64	57	64	65
BamB	19	17	13	23	19	100	65	66	65
CmsB	16	20	17	16	17	34	100	65	62
SaciB	23	19	15	25	24	28	20	100	68
PagB	21	21	14	23	25	21	23	31	100

B

BalhA1 MEQKILDIKLTETGKINYAHKPDDSGCAGCMGCAGGTGCAGTGCIGQGVWKKCSGK
 BalhA2 MEQKKSLEIKLTESGKIDYAHKPDDSGCAACIGTTSCGGVDPTKPGIWKRCSSK
 BcerA MEQKKSLEIKLTESGKINYAHTPDSPGCAGGCVGTTSCTGVDPKPGVWQRCSGK
 BamA MEEVTIMTQIKVPTALIASVHGEQHLFEPMAARCTCTTIISSSSTF
 CmsA MESGAPAPLRTTATEVAPAAGDDASDALLAEAFGFTITHRGAEELVMGDVTLCCSTTCSSSGGGRQQR
 McbA MELKASEFGVVLSDALKLSRQSPPLGVGIGGGGGGGGGSCGGQGGCGGCSNGCSGGNGGSGGSGSHI
 PagA MVEGFKFEIFEYEEGPILPLDDDDPIIIACCCGGGGDNWKIFSTKPNP
 SaciA MRAYYTVRRANLIYQAYSEGRVLFVWFGWFGWFGGGGRVSG

Figure S1. Dehydrogenase identity/similarity matrix and amino acid sequence of precursor peptides. **A.** Amino acid percent similarity (blue) and percent identity (green) matrix between dehydrogenases of interest to this study. ClustalW2 was used to calculate the pairwise identities and similarities.¹ **B.** Amino acid sequence of the cognate precursor peptide(s) for each dehydrogenase utilized in this study. Known residues to be cyclized *in vivo* or *in vitro* are colored red. Only the BalhA1 and McbA precursor peptides were used in this study.

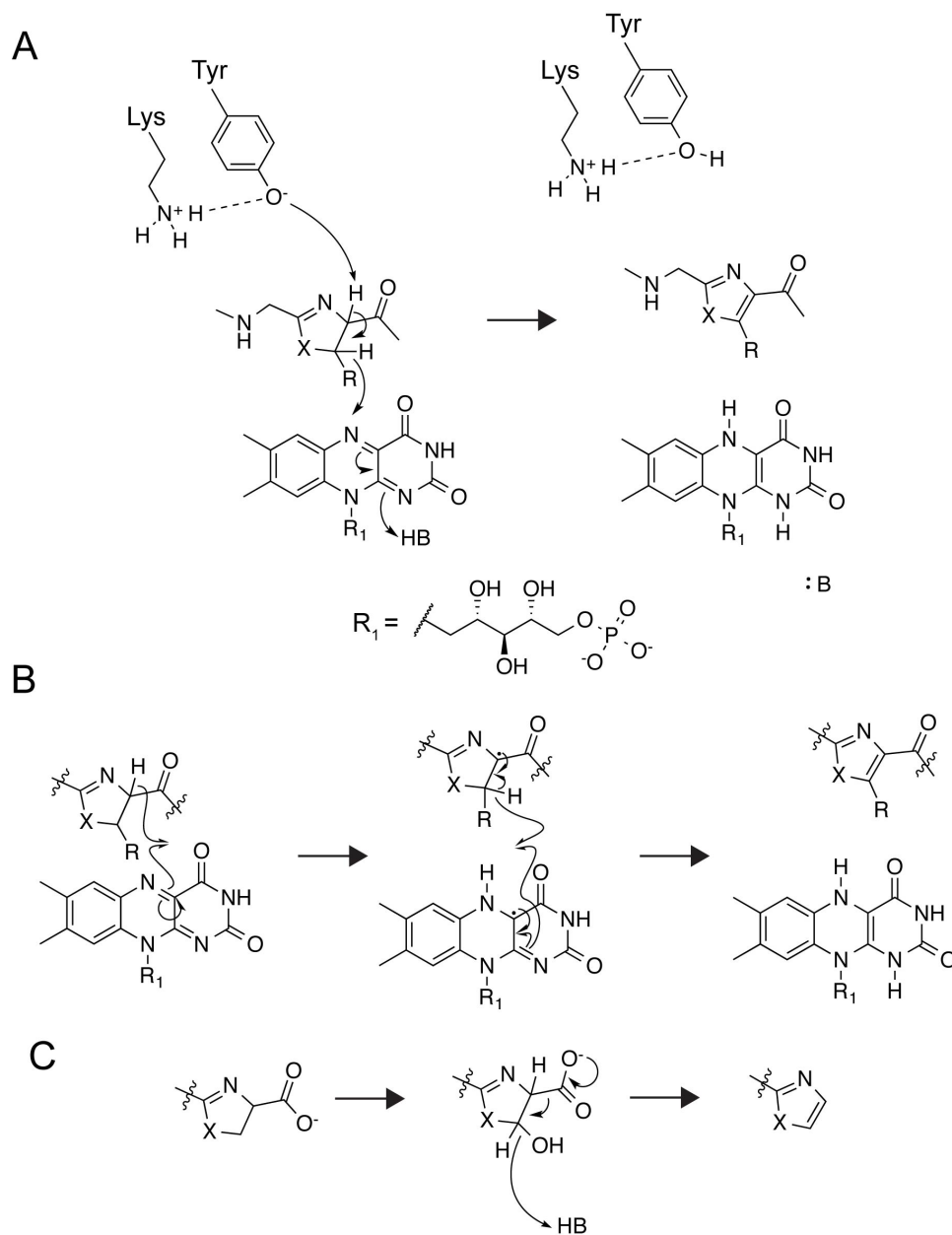


Figure S2. Three potential pathways for azole formation in ribosomal natural product biosynthesis. A. A possible polar mechanism for azoline dehydrogenation, which implicates the conserved Lys-Tyr motif in acid/base catalysis. **B.** Alternative radical mechanism for dehydrogenation that proceeds via a semiquinone radical intermediate. The data in this paper do not distinguish between the mechanisms drawn in panel A/B. **C.** Hypothesized oxidative decarboxylation mechanism for thiazole formation in the natural product bottromycin.²⁻⁴ The bottromycin biosynthetic gene cluster lacks a bioinformatically identifiable TOMM dehydrogenase. Cys: X = S, R = H; Ser: X = O, R = H; Thr: X = O, R = CH₃.

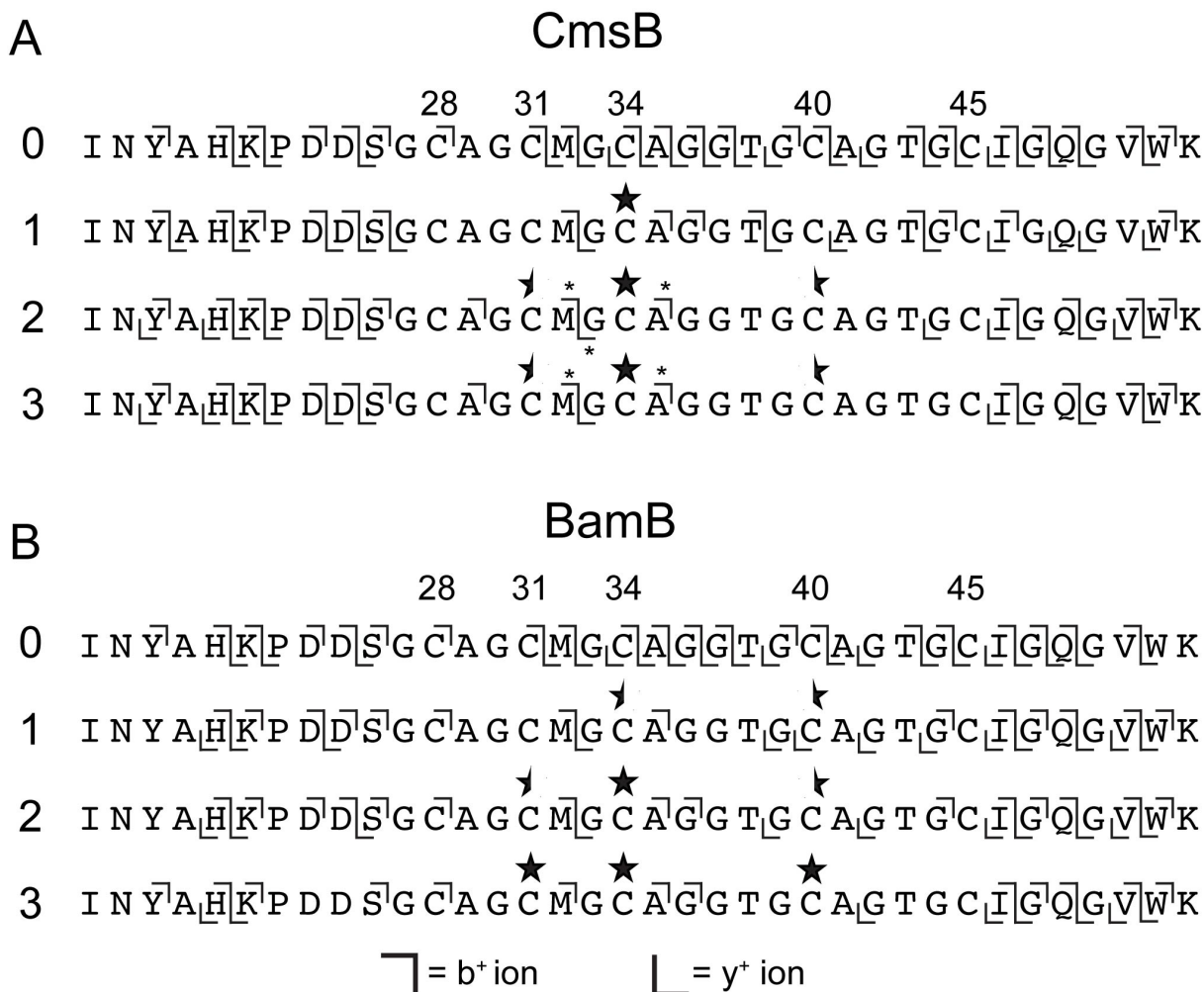


Figure S3. The order of azole formation on BalhA1-5Tzn by CmsB and BamB. A. Synthetase reactions containing BalhA1-5Tzn treated with CmsB were quenched by the addition of trypsin and subjected to LC-FTMS/MS. The fragment ions observed for various ring intermediates are denoted by the b⁺ and y⁺ ion symbols. The leftmost numbers indicate ring state. Across the top, cysteines are numbered based on the sequence of full length BalhA1. Stars signify thiazole locations. A half star signifies that there are ions indicative of a thiazole as well as a free cysteine at that position. Asterisks denote ions containing a mixed population of two peptides. **B.** Same as **A** except using BamB.

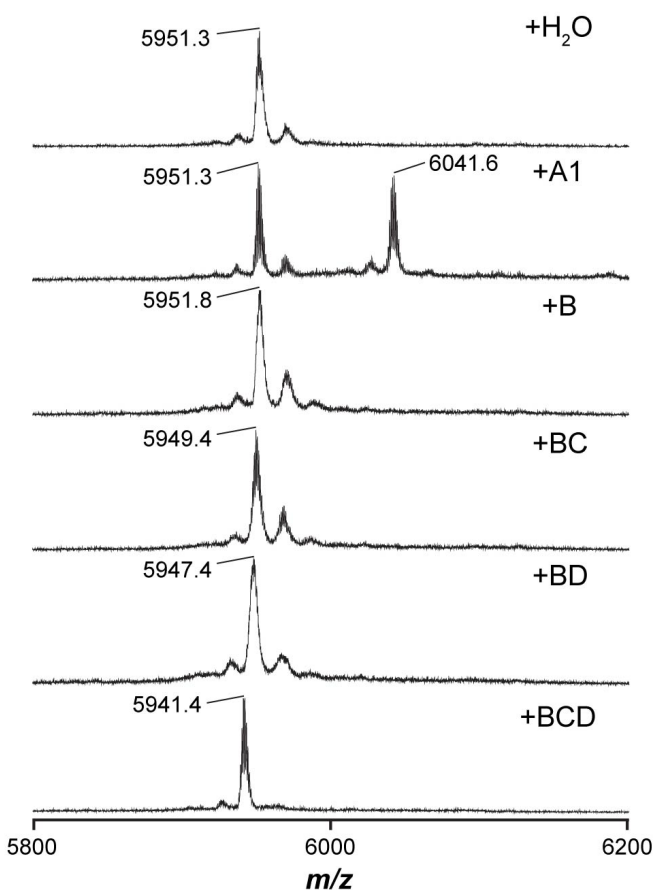


Figure S4. Minimal requirement for dehydrogenase activity. BalhA1-5Tzn was treated with various components of the TOMM synthetase. All samples contained supplemental FMN (50 μ M). The reactions were allowed to react for 16 h at 25 °C prior to analysis by MALDI-TOF-MS. During the preparation of BalhA1-5Tzn, BalhC/D were precipitated using acetonitrile. To demonstrate that all of the BalhC/D had been removed or inactivated, additional BalhA1 was added to a reaction (+A1), and remained unmodified after the reaction (m/z 6041). This suggests that the processing seen for the subsequent reactions was the result of the indicated proteins. The addition of BcerB alone to BalhA1-5Tzn (+B) did not result in any azole formation, evidenced by the lack of mass shift (m/z 5951). Addition of BcerB, in conjunction with BalhC (+BC) or BalhD (+BD), resulted in 1 thiazole or 2 thiazoles as the major species (m/z 's 5949, 5947 respectively). However, efficient dehydrogenation only occurred when BcerB, BalhC, and BalhD were all present, as evidenced by the loss of 10 Da (5 x 2H, m/z 5941). To remove any unmodified thiazoline heterocycles, all the reactions were hydrolyzed and analyzed again using MALDI-TOF-MS (Figure 8).

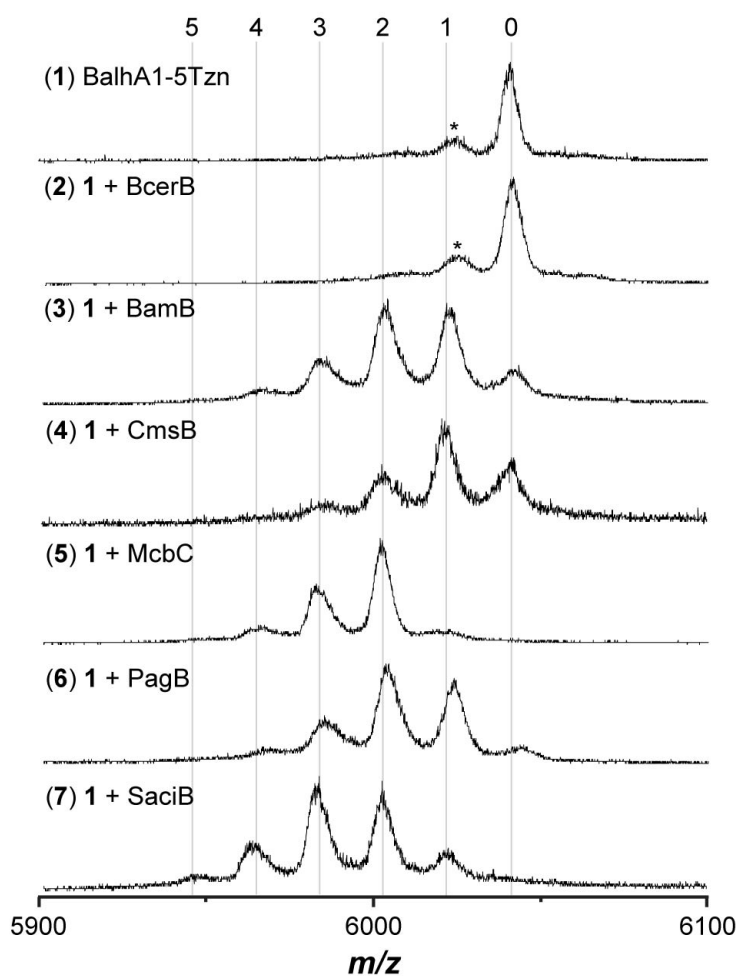


Figure S5. Noncognate dehydrogenase activity towards BalhA1-5Tzn. BalhA1-5Tzn and various dehydrogenases were allowed to react for 16 h at 25 °C. To remove any unreacted thiazoline heterocycles, formic acid (10% v/v) was added and allowed to react for at least 1 h prior to MALDI-TOF-MS analysis. The numbers above the spectra indicate the number ofazole heterocycles. The asterisk denotes a laser-induced artifact.

BalhB	FNNRKSVE-ELEIRTRISFEKLSNLLHFSYGYVNK-----EHNVAPSAGAKYP	118
BcerB	LNNRKSVE-ELEIRTRIRFETLSNLLHFSYGYINK-----PHSAAPSAGGKYP	117
McbC	VINISSSHNFSRERLPSGINFCDNKLSIRTIEKLLVNAFSSPDGVSRRPYPSGGALYP	139
CmsB	LAARRSAEPR-TLGRPVELAELATVLRLAYGPR-G-----DGTPRRFVPSGGGLYP	170
BamB	IQNRRSIE-Q-FNGGSTTLAQLSTILQGSYGLIER-----PEGPRRPPIPSGGALYP	138
PagB	IVTRRSIR-T-FSYEPIKLNELSVLLKLSGGVLI----QDEENHSIYHRSFPTAGGLNS	138
SaciB	MKRRHSR-A-FRRERINLNKISSLLWYSVGVEI-----ENGIQFRMFPSAGNLAE	105
	: * : : * :	*:.*
BalhB	ISIIYIVIFNVE--NL--EQGIYYNKEQDTLELIRKGEYR---DAINNLY-----IDNNH	166
BcerB	INIYIAVFNVE--NL--EQGIYYDREQDVLDMIRRGDFR---ESINNLY-----VDNTH	165
McbC	IEVFLCRLSENTENWQAGTNVYHYLPLSQALEPVATCNTQ-----SLYRSLSGGDSER	192
CmsB	LDLHVVARSVV--GL--EPGIHQLDPLEETLVDSGLDRD---GQLARFRRRAAPSLMAPI	223
BamB	LDLYVVSNKVD--SL--EKGLYHFDPYRKGLVHLGEYSEE---DFGRIML-----QEEA	185
PagB	CHVYLISLNVDD--DL--PFGSYYDPLTHELIKIEEYQISQKNEFLDTLVKVLG--NQEW	192
SaciB	TEVYLISLYT---DL--EKGVYHYDPVEGSLDVLSNDL-D-EELMLQAIK---N--SLPD	153
	::: : * :	:
BalhB	IHSSSFIMFHVADLNKTSNKYEDRGYKLIHLDMGHLSQNLVLLSSAQQLGIRAIIFGLYEN	230
BcerB	IHSSSFIMFHAANLDQTSSKYADRGYKLIHLDMGHLSQNLVLLSSAQQLGIRAIIFGLYEN	229
McbC	LGKPHFALVYCIIFEKALFKYRYRGYRMALMETGSMYQNAVLVADQIGLKNRVWAGYTDS	256
CmsB	PETAAVTVVITGSFERSRCKYGLRGYRLTLEAGHVGQNALLVATALGLPVLGWVGFVDH	287
BamB	VKDFSFAVIISASFWRSRFKYGHRSYRFIFIEAGHLMQNMILLATAQCIQSRPYGGFIDD	249
PagB	IRTAGLILIIITGDYSKIRLKYGDRGYRYLLEAGHIMQNFYLIASMLNLGVCISIGGFYDD	256
SaciB	ITFVPLIILLTSLYWKPMVKTGNRGARFSLIDTGIVIEINFYLVATALGLGISAIIGGFNDD	217
	. :. : ** * . : : * : * * : :	* :
BalhB	KVNEFLEI-DGENEFVLLSH-VFGGIKYPTPVTMDTKFSDIYYENEIESE-	279
BcerB	KVNDFLEL-DGENEFVLLSH-VFGGIKLSTPITMDTKFSDIYYENEETKSEG	279
McbC	YVAKTMNL-DQRTVAPLIVQ-FFGDVNDDK-CLQ-----	287
CmsB	ELDAV-LGLDGVTOSSLYAI-SFGGADPGARRFADEEASHD-----	326
BamB	ELMDLIGGHNGVDDAPIYTL-VAGT-----	273
PagB	YIAKLIHV-DNTNELVLY-LGGMGKLV-----	281
SaciB	FFNKLIGV-GMEKGEVVIGMLVVGEE-----	242
	.	

Figure S6. Multiple sequence alignment of TOMM dehydrogenases. The dehydrogenases used in this study were aligned using ClustalW2.¹ A known FMN-binding motif is highlighted in yellow, which is lacking in McbC. The invariant Lys-Tyr motif originally identified in a previous study is highlighted in green.⁵ Residues mutated in this study are colored red.

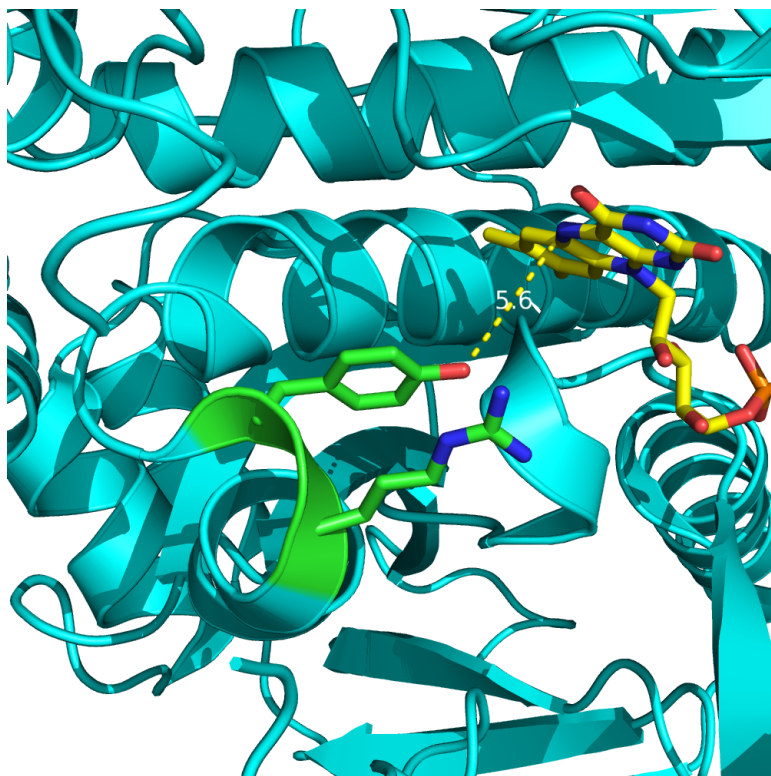


Figure S7. Non-TOMM dehydrogenase crystal structure highlighting the Lys-Tyr motif. A ribbon diagram of a putative nitroreductase from *Anabaena variabilis* ATCC 29413 (PDB entry 3EO7). The TOMM dehydrogenase Lys-Tyr motif aligns to 3EO7-R175 and -Y176, whose side chains are shown in stick with green carbons. The FMN cofactor is also shown in stick but with yellow carbons. The closest distance between R175 and Y176 and the FMN cofactor is displayed as a yellow dotted line and was measured to be 5.6 Å.

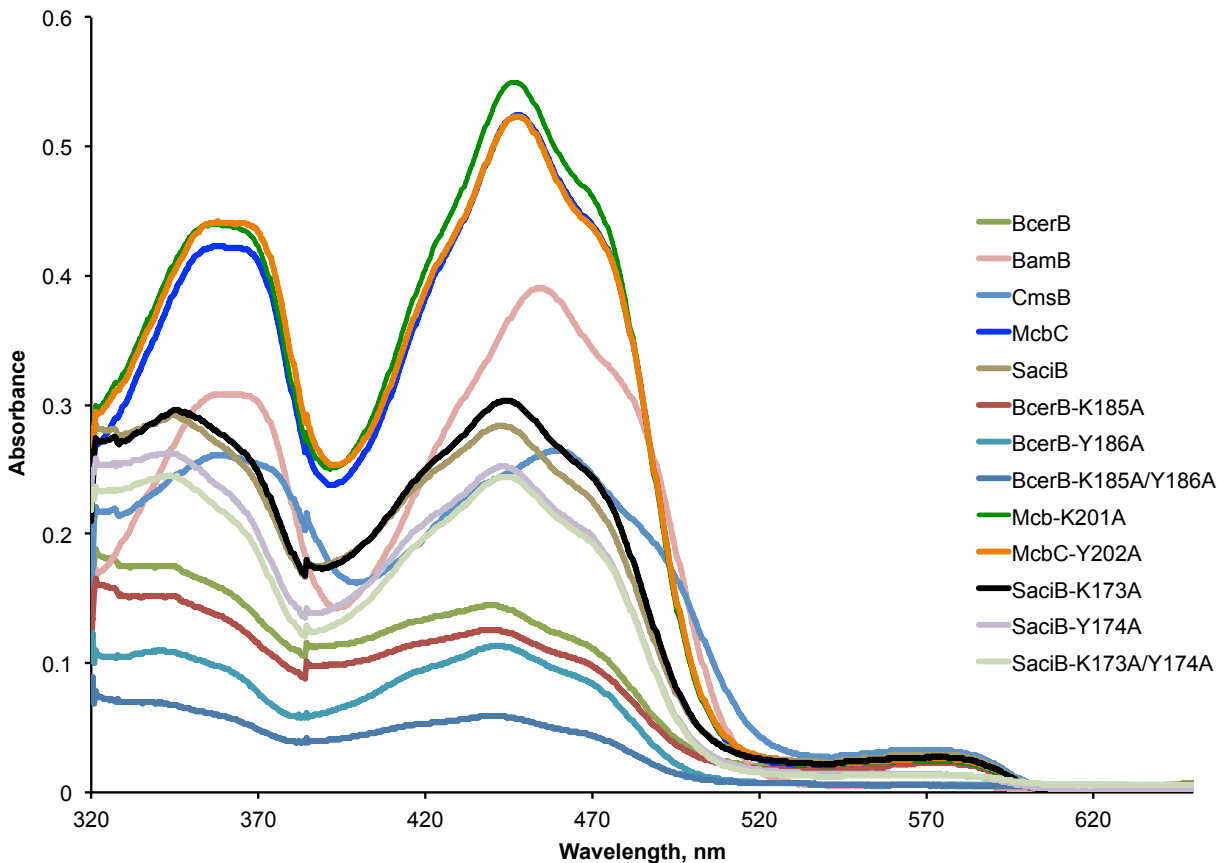


Figure S8. UV/Vis spectra of TOMM dehydrogenases. A UV/Vis spectrum for each dehydrogenase used in this study was collected at 50 μM total protein concentration. The intensity of the FMN peaks ($\lambda_{\text{max}} = 440\text{-}460$ nm) reflects the FMN content after heterologous expression and purification from *E. coli* for a particular dehydrogenase. Based on the molar absorptivity of FMN ($12,500 \text{ M}^{-1} \text{ cm}^{-1}$), a dehydrogenase with 100% loading would have an absorbance of 0.625 at λ_{max} . The subtle inconsistency in the shape of the spectra at 380 nm is due to a source changeover (deuterium UV lamp to Vis lamp) within the spectrophotometer.

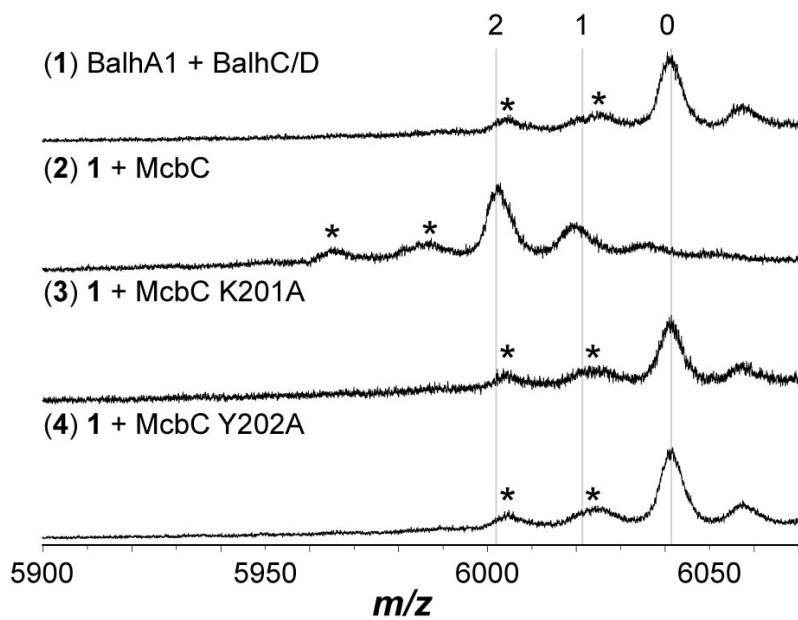


Figure S9. McbC-K201A and -Y202A lack dehydrogenase activity. Synthetase reactions containing either wild-type McbC or the indicated mutant proceeded for 16 h at 25°C. Subsequently, all azolines were hydrolyzed by acidification with formic acid prior to MALDI-TOF-MS analysis. Asterisks denote laser-induced artifacts. The numbers above the spectra indicate the number of azoles.

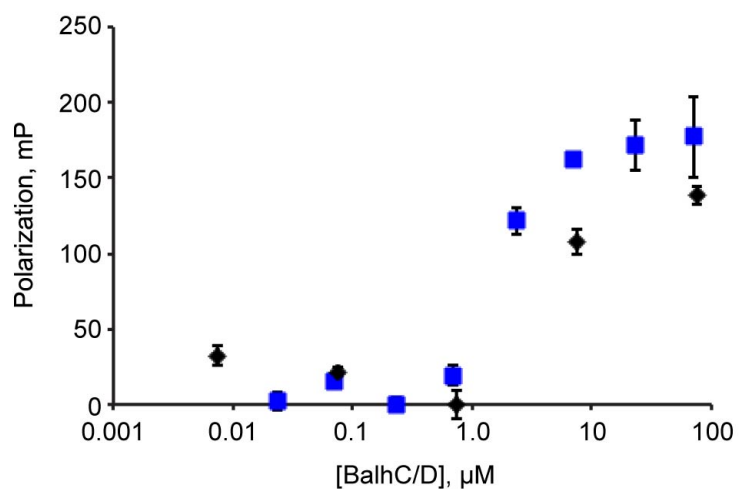


Figure S10. Binding of BcerB-K185A/Y186A to BalhC/D. The fluorescence polarization of the FMN cofactor of BcerB-K185A/Y186A ($1 \mu\text{M}$) was measured with varying concentrations of the BalhC/D (black). The binding curve for wild-type BcerB is shown in blue. These data indicate that the Lys-Tyr motif is not integral for synthetase complex formation as evidenced by a highly similar binding curves upon comparison to wild-type BcerB. The point of lowest polarization for BcerB-K185A/Y186A and BcerB were normalized to 0 mP. The error reported for each individual data point corresponds to the standard deviation of three technical replicates.

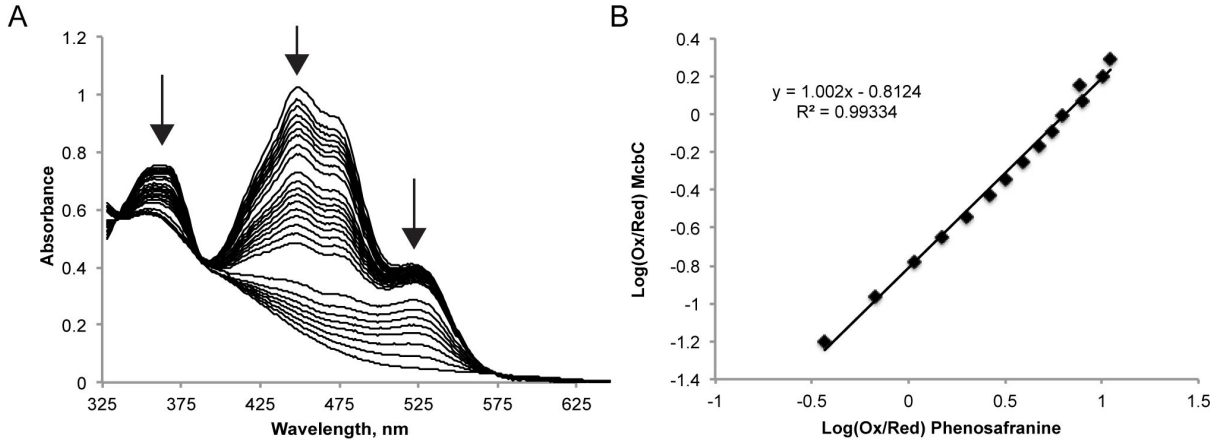


Figure S11. The reduction potential of McbC as measured by phenosafranine titration. A, Upon chemical reduction of the FMN cofactor by sodium dithionite, the visible absorbance of McbC was decreased (arrows). The absorbance at 525 nm arises from the presence of the redox indicator dye, phenosafranine, which also loses visible absorbance upon reduction. **B,** The fraction of oxidized (ox) and reduced (red) flavin and phenosafranine were calculated from the spectra shown in panel A. The reduction potential of the dehydrogenase was calculated from the y-intercept by plotting the log(ox/red) BcerB versus the log(ox/red) for phenosafranine.⁶ Since the reduction of phenosafranine is a two-electron process, a slope of one indicates that the reduction of the FMN cofactor in McbC involves two electrons.

References

1. Larkin, M. A., Blackshields, G., Brown, N. P., Chenna, R., McGettigan, P. A., McWilliam, H., Valentin, F., Wallace, I. M., Wilm, A., Lopez, R., Thompson, J. D., Gibson, T. J., and Higgins, D. G. (2007) Clustal W and Clustal X version 2.0, *Bioinformatics* 23, 2947-2948.
2. Crone, W. J. K., Leeper, F. J., and Truman, A. W. (2012) Identification and characterisation of the gene cluster for the anti-MRSA antibiotic bottromycin: expanding the biosynthetic diversity of ribosomal peptides, *Chem. Sci.* 3, 3516-3521.
3. Gomez-Escribano, J. P., Song, L. J., Bibb, M. J., and Challis, G. L. (2012) Posttranslational beta-methylation and macrolactamidation in the biosynthesis of the bottromycin complex of ribosomal peptide antibiotics, *Chem. Sci.* 3, 3522-3525.
4. Huo, L., Rachid, S., Stadler, M., Wenzel, S. C., and Muller, R. (2012) Synthetic biotechnology to study and engineer ribosomal bottromycin biosynthesis, *Chem. Biol.* 19, 1278-1287.
5. Dunbar, K. L., Melby, J. O., and Mitchell, D. A. (2012) YcaO domains use ATP to activate amide backbones during peptide cyclodehydrations, *Nat. Chem. Biol.* 8, 569-575.
6. Massey, V. (1991) A simple method for the determination of redox potentials, In *Flavins and Flavoproteins* (Curti, B., Ronchi, S., and Zanetti, G., Eds.) pp 59-66, Walter de Gruyter, Como, Italy.